https://doi.org/10.15407/ujpe64.3.197

R. HAZRA, MD.M. HOSSAIN

Department of Physics, Aliah University
*(II A/27, New Town, Kolkata-700160, India; e-mail: mhossain.phy@gmail.com, mhossain.phys@aliah.ac.in)*

# STUDY OF ATOMIC POPULATIONS, ELECTROMAGNETICALLY INDUCED TRANSPARENCY, AND DISPERSIVE SIGNALS IN A Λ-TYPE SYSTEM UNDER VARIOUS DECOHERENCE EFFECTS

*We have theoretically studied the atomic populations, electromagnetically induced transparency (EIT), and dispersion in a three-level Λ-type system. The density matrix equations are set up with regard for the relaxation of populations of the ground states, and the optical Bloch equations are solved analytically in the weak probe field approximation. Decoherence effects in the ground and excited states on the EIT line shape and dispersive signals are studied, and it is found that the EIT line width increases and the peak height decreases, as the decoherence rates increase in the ground and excited states. On the other hand, we have observed that the dispersive signals are steeper and of high contrast for the lower decoherence rates in the ground and excited states. We have also analyzed the variations of atomic populations of the energy levels at the pump Rabi frequency, as well as the decoherence rate in the ground state.*

*K e y w o r d s*: electromagnetically induced transparency, dispersion, decoherence, density matrix, lambda-type system.

## 1. Introduction

Atomic coherence and interference effects in an atomic medium that interacts with two or more laser fields produce some interesting coherent resonances like electromagnetically induced transparency (EIT) [1–4] and electromagnetically induced absorption (EIA) [5–8]. The coherent phenomenon, EIT, is a laser-induced quantum interference effect, in which an absorbing medium becomes transparent, when the two laser fields (one weak laser field, "probe laser" and another strong laser field, "pump laser") satisfy the two-photon Raman resonance condition in a three-level lambda- (Λ) or vee- (V) or (Ξ) cascade-type system. In a three-level Λ-type system, the pump and probe laser fields are connected to a common excited hyperfine level from two ground hyperfine levels (Fig. 1). Recently, the EIT has drawn a lot of attention due to its vast ranges of applications in atomic clock [9], slow light [10–11], light storage [12], quantum information and computation [13], precision magnetometer [14], *etc.* The EIT resonance has attracted a greater attention due to its narrow spectral line width. So, we have to understand the various coherent and incoherent phenomena responsible for the narrowing and broadening of an EIT line width, respectively. Many authors [15–29] have studied both theoretically and experimentally the narrowing and broadening effects on the EIT line width. In the case of the broadening of EIT line width, various decoherence effects present in a real atomic system play an important role. Decoherence in EIT is caused by several mechanisms such as the population exchange be-

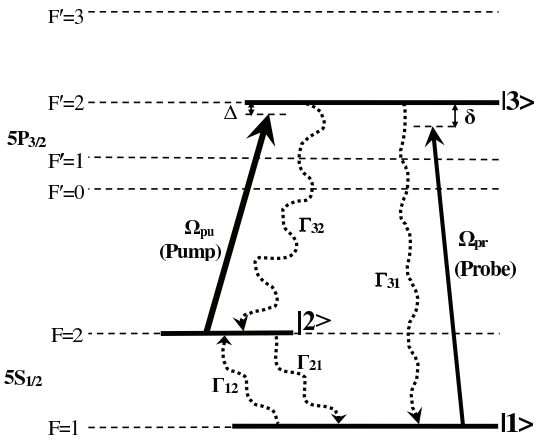


***Fig. 1.*** Energy level diagram of a three-level Λ-type EIT system in the hyperfine transitions of $^{87}$Rb-D$_2$ line. $\Omega_{pu}$ and $\Omega_{pr}$ are the pump and probe Rabi frequencies, respectively. $\Gamma_{ij}$ are the population decay rates between the levels $|1\rangle$, $|2\rangle$ and $|3\rangle$ $(i, j = 1, 2, 3;\ i \neq j)$

tween energy levels, atom-atom and atom-wall collisions, laser line width fluctuation, transit time broadening, spin exchange collisions, *etc.* [19–31, 32–34].

In the case of a Λ-type EIT system, the radiative transitions among the ground hyperfine levels are usually forbidden. So, the atomic coherence can be preserved in between the ground hyperfine levels for a long time. As a result, the spectral line width of the EIT resonance in a Λ-type system is primarily determined by the inverse lifetime of an atom in the coherent superposition of the ground hyperfine levels. In Refs. [19–28], the authors have studied the EIT resonances under various decoherence effects arising in the ground states and observed that the EIT line shape gets affected due to the dephasing of ground states, population relaxation between the ground states, laser line width fluctuation, and buffer gas-induced collisional dephasing in the ground states. Figueroa *et al.* [25] showed that the dephasing in the ground states plays the dominant role of decoherence in EIT, while the population exchange plays a minor role. At the same time, Javan *et al.* [16] assumed in their work that the population exchange is the major source of decoherence in EIT. In Refs. [19, 23, 26–28, 31], the authors have considered the effect of decoherence arising from both the population exchange and dephasing in the ground states. In few papers [23, 24], we have also found that the laser line width fluctuation causes an additional population relaxation between the ground states. On the other hand, the introduction of a buffer gas in an atomic vapor cell can prolong the interaction time between the atoms and the laser field, which increases, in turn, the ground-state coherence rate. Many authors [15, 19–23, 32–35] have studied both theoretically and experimentally the buffer gas-induced narrow spectral line width of EIT. But, at the same time, a few authors [19–21] showed that the presence of a buffer gas increases the dephasing rate from the excited levels along with the increase of ground-state coherence rates.

In addition to the ground-state decoherence effects on EIT, a few authors studied [20–23, 28, 29] the EIT line shapes under various excited state decay rates along with the spontaneous decay rates from the excited states. In a real atomic medium (say, Rb vapor in a cell), the coherence lifetime is usually determined by the interaction time of atoms and laser beams. This interaction time may be reduced by various excited state decoherence phenomena like the excited atom-atom collision, laser field fluctuation, non-radiative decays between neighboring excited levels, buffer gas-induced collision with the atoms, *etc.* In Refs. [20, 21, 28], the authors showed that the higher buffer gas pressure produces a broadening of the excited states (i.e., the decoherence of excited states increases) and, at the same time, restricts the further diffusion of atoms resulting in a decrease of ground state decoherence rates. Erhard *et al.* [23] also considered the effect of laser line width fluctuations as another source of decoherence for the excited levels. Moreover, the non-radiative decay rates between the neighboring hyperfine excited levels may increase the excited state decoherence rates [29].

The real part of a probe field is directly related to the real part of the nonlinear susceptibility $(\chi)$ which represents the dispersion of a medium. The dispersive property of an atomic medium is greatly modified due to a narrow EIT signal to the probe field. The EIT window exhibits a reduced absorption feature at the line center of the probe spectrum. At the same time, it has narrow line width. These two characteristics of the EIT signal result in the rapidly increasing refractive index near the line center. As a result, the group velocity of a light pulse propagating in the EIT medium is reduced remarkably. This normal dispersion of the EIT medium has interesting applications in the field of nonlinear optics like a "slow

light", storage of light pulses [4, 37, 38], *etc.* In 1992, Harris *et al.* [39] theoretically showed that the EIT phenomenon can be used for a reduction of the group velocity, i.e., for the production of a "slow light". The key ingredient for the slow-light effect is to find out a very narrow EIT window to the probe field. We have discussed earlier that the narrow and high-contrast EIT signal is affected by both the ground and excited decoherence effects. So, the various decoherence effects also affect the dispersive signals. Therefore, the various decoherence effects on the dispersion signal also affect a reduction of the group velocity or slow-light effect.

In this article, we will consider a quasistationary solution of the density matrix equations for a three-level Λ-type EIT system under two co-propagating laser fields, where the solution is performed analytically in a weak probe approximation. We have studied theoretically the line shapes of both probe absorption and dispersion signals in a three-level Λ-type EIT system under various decoherence effects arising from both the ground and excited states. In the case of ground state decoherence phenomena, we will discuss the dephasing of ground states, population relaxation between ground states, laser line width fluctuations, and buffer gas-induced collisional dephasing. We will study the various decoherence effects arising in the excited states such as buffer gas-induced collisional effects, laser line width fluctuations, and other non-radiative decays. In addition to the decoherence effects, we consider variations of the atomic populations of energy levels with the pump Rabi frequency and the ground state decoherence rates. Finally, the effect of the pump detuning on the EIT line shapes and the effect of a buffer gas on the coherence preservation will be discussed.

## 2. Theory

Consider a three-level Λ-type system formed by two ground hyperfine levels $|1\rangle$ ($F = 1$) and $|2\rangle$ ($F = 2$) and a common excited hyperfine level $|3\rangle$ ($F' = 2$) in the hyperfine transitions of $^{87}$Rb-$D_2$ line (Fig. 1). A strong pump laser field at the Rabi frequency $\Omega_{pu}$ is coupled to the transition $|2\rangle \to |3\rangle$ with a frequency detuning $\Delta = \omega_{32} - \omega_{pu}$, and a weak probe laser field at the Rabi frequency $\Omega_{pr}$ is connected to the transition $|1\rangle \to |3\rangle$ with a frequency detuning $\delta = \omega_{31} - \omega_{pr}$, where $\omega_{32} = (E_3 - E_2)/\hbar$ and $\omega_{31} = (E_3 - E_1)/\hbar$ are the hyperfine transition frequencies between the levels $F = 2 \to F' = 3$ and $F = 1 \to F' = 3$, respectively; $\omega_{pu}$ and $\omega_{pr}$ are the angular frequencies of the pump and probe lasers, respectively (Fig. 1). The Rabi frequencies, $\Omega_{pu}$ and $\Omega_{pr}$ are defined as $\Omega_{pu} = -\mu_{23}E_{pu}/\hbar$ and $\Omega_{pr} = -\mu_{13}E_{pr}/\hbar$, where $\mu_{23}$ and $\mu_{13}$ are the atomic dipole moments for the transitions $|2\rangle \to |3\rangle$ and $|1\rangle \to |3\rangle$, respectively; $E_{pu}$ and $E_{pr}$ are the electric field amplitudes of the pump and the probe laser fields, respectively. The population relaxation rates between the levels $|1\rangle$, $|2\rangle$, and $|3\rangle$ are defined by $\Gamma_{ij}$ (where $i, j = 1, 2, 3$; $i \neq j$). As per the selection rule $\Delta F = 0, \pm 1$, the pump laser can connect the hyperfine levels $F = 2 \to F' = 1, 2, 3$, and the probe laser can connect the hyperfine levels $F = 1 \to F' = 0, 1, 2$. Therefore, the two levels $F' = 1$ and $F' = 2$ are the common levels for both the pump and probe lasers. Now to realize a theoretical model of the three-level Λ-type system, we have taken $F' = 2$ as a common excited level to the pump and probe lasers, because the energy level $F' = 2$ is far away from the levels $F' = 0$ and 1. It is worth to note that the energy separation of $F' = 1$ and 2 is almost twice higher than the energy separation of $F' = 0$ and 1.

We set up the density matrix equations for a three-level Λ-type system, by using the Liouville's equation of motion and taking the various relaxation rates into account. In the rotating wave approximation (RWA), the following optical Bloch equations are obtained [1, 18, 36]:

$$\dot{\rho}_{11} = \frac{i\Omega_{pr}(\rho_{31} - \rho_{13})}{2} + \Gamma_{31}\rho_{33} + \Gamma_{21}\rho_{22} - \Gamma_{12}\rho_{11}, \quad (1)$$

$$\dot{\rho}_{22} = \frac{i\Omega_{pu}(\rho_{32} - \rho_{23})}{2} + \Gamma_{32}\rho_{33} + \Gamma_{12}\rho_{11} - \Gamma_{21}\rho_{22}, \quad (2)$$

$$\dot{\rho}_{33} = \frac{-i\Omega_{pr}(\rho_{31} - \rho_{13})}{2} - \frac{i\Omega_{pu}(\rho_{32} - \rho_{23})}{2} - (\Gamma_{31} + \Gamma_{32})\rho_{33}, \quad (3)$$

$$\dot{\rho}_{31} = -(i\delta + \gamma_{31})\rho_{31} + \frac{i\Omega_{pu}\rho_{21}}{2} - \frac{i\Omega_{pr}(\rho_{33} - \rho_{11})}{2}, \quad (4)$$

$$\dot{\rho}_{32} = -(i\Delta + \gamma_{32})\rho_{32} - \frac{i\Omega_{pu}(\rho_{33} - \rho_{22})}{2} + \frac{i\Omega_{pr}\rho_{12}}{2}, \quad (5)$$

$$\dot{\rho}_{21} = -[i(\delta - \Delta) + \gamma_{21}]\rho_{21} + \frac{i\Omega_{pu}\rho_{31}}{2} - \frac{i\Omega_{pr}\rho_{23}}{2}. \quad (6)$$

Here, we have introduced two categories of decay rates. The first is the population relaxation rate ($\Gamma_{ij}$),

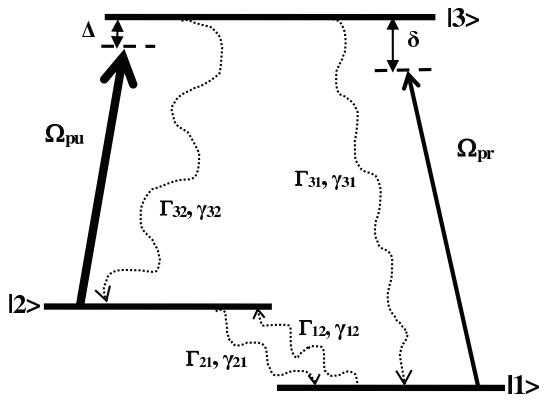


***Fig. 2.*** Representation of various decay rates; $\Gamma_{ij}$ are the atomic population relaxation rates, and $\gamma_{ij}$ are the atomic coherence relaxation rates

and the second is the coherence relaxation rate ($\gamma_{ij}$) (Fig. 2). In Fig. 2, we have considered the atomic population relaxation rates between the $|i\rangle^{th}$ and $|j\rangle^{th}$ levels as $\Gamma_{21} = \Gamma_{12} = \Gamma_{pe}$ and $\Gamma_{31} = \Gamma_{32} = \Gamma$ (where $\Gamma/2\pi$ is the natural line width (6.0 MHz) of the excited level $5P_{3/2}$ of a Rb atom) and the coherence relaxation rates between the $|i\rangle^{th}$ and $|j\rangle^{th}$ levels as $\gamma_{32} = \frac{\Gamma_{31}+\Gamma_{32}+\Gamma_{21}}{2} = \frac{2\Gamma+\Gamma_{pe}}{2}$, $\gamma_{31} = \frac{\Gamma_{31}+\Gamma_{32}+\Gamma_{12}}{2} = = \frac{2\Gamma+\Gamma_{pe}}{2}$ and $\gamma_{21} = \gamma_{12} = \gamma_{dp}$.

The density matrix equations (1)–(6) are analytically solved under the assumption of a strong pump beam and a weak probe beam so that the atomic population primarily remains in the ground states, and we get the steady-state solution related to the probe transition as

$$\rho_{31} = \left[\left\{\frac{i\Omega_{pr}\{\Gamma\Gamma_{pe}\Omega_{pu}^2\}}{(\gamma_{32}-i\Delta)(3D\Gamma_{pe}+D\Gamma+4\Gamma\Gamma_{pe})} + \right.\right.$$

$$\left.\left. + \frac{2i\Omega_{pr}[i(\delta-\Delta)+\gamma_{dp}](D\Gamma+2\Gamma\Gamma_{pe})}{(3D\Gamma_{pe}+D\Gamma+4\Gamma\Gamma_{pe})}\right\}\Big/ \right.$$

$$\left.\Big/\{4\{(i\delta+\gamma_{31})[i(\delta-\Delta)+\gamma_{dp}]\}+\Omega_{pu}^2\}\right], \qquad (7)$$

where $D = \frac{\Omega_{pu}^2\gamma_{32}}{2(\Delta^2+\gamma_{32}^2)}$.

If we consider the case where the pump laser frequency is exactly locked to the transition $|2\rangle \to |3\rangle$, then the value of the pump detuning ($\Delta$) becomes zero. Therefore, at $\Delta = 0$, Eq. (7) becomes

$$\rho_{31} = \left[\left\{\frac{i\Omega_{pr}\{\Gamma\Gamma_{pe}\Omega_{pu}^2\}}{\gamma_{32}(3D_0\Gamma_{pe}+D_0\Gamma+4\Gamma\Gamma_{pe})} + \right.\right.$$

$$\left.\left. + \frac{2i\Omega_{pr}[i(\delta+\gamma_{dp})](D_0\Gamma+2\Gamma\Gamma_{pe})}{(3D_0\Gamma_{pe}+D_0\Gamma+4\Gamma\Gamma_{pe})}\right\}\Big/ \right.$$

$$\left.\Big/\{4\{(i\delta+\gamma_{31})[i(\delta+\gamma_{dp})]\}+\Omega_{pu}^2\}\right], \qquad (8)$$

where $D_0 = \frac{\Omega_{pu}^2}{2\gamma_{32}}$.

In this work, we have considered that the imaginary and real parts of the coherence term between the levels coupled by the probe field are proportional to the probe absorption and probe dispersion signals, respectively. Therefore, $\mathrm{Im}(\rho_{31})$ is directly proportional to the probe transmission signal, and the EIT resonance is obtained in the probe scanning signal under the two-photon Raman resonance condition ($\delta - \Delta = 0$). At the same time, $\mathrm{Re}(\rho_{31})$ is directly proportional to the probe dispersion signal. We have plotted both $\mathrm{Im}(\rho_{31})$ and $\mathrm{Re}(\rho_{31})$ as functions of the probe frequency detuning ($\delta$) under various decoherence effects and analyzed the EIT line shapes and dispersion signals. We have considered the fixed values of $\Omega_{pu}/(2\pi) = 5.0$ MHz, $\Omega_{pr}/(2\pi) = 0.1$ MHz, and $\Gamma/(2\pi) = 6.0$ MHz. All the numerical values of the various decoherence rates are taken within the ranges of available data in papers [19–31].

## 3. Results and Discussion

We present the results of our study of various decoherence effects on the EIT and dispersive signals in two subsections: (3.1) Ground-state decoherence effects and (3.2) Excited state decoherence effects. The effects of various parameters on the atomic populations are presented in subsection (3.3).

### *3.1. Ground-state decoherence effects*

In the case of a $\Lambda$-type EIT system, the radiative transition among the ground hyperfine levels ($F = 1$ and $F = 2$ for $^{87}$Rb-$D_2$ line) is forbidden, so the atomic coherence in the ground hyperfine levels can be preserved for a long time. But this atomic coherence may be affected by various physical phenomena occurring in the atomic medium such as elastic and inelastic atom-atom and atom-wall collisions, temperature fluctuations, flight through broadening, laser line width fluctuations, *etc.* [19, 23–28, 31]. There is a belief existing among many researchers that the ground-state decoherence effects mainly arise from the elastic and inelastic atom-atom and atom-wall

collisions [25, 26]. But we study all physical phenomena mentioned above to observe various ground-state decoherence effects on the EIT and dispersive signals. We plot the probe transmission $\{\mathrm{Im}(\rho_{31})\}$ and dispersion $\{\mathrm{Re}(\rho_{31})\}$ signals as a function of the probe detuning ($\delta$) in Figs. 3(i) and 3(ii), respectively, to study the various ground-state decoherence effects. Here, we have used Eq. (8), and the various ground-state decoherence rates are incorporated in $\Gamma_{pe}$, $\gamma_{dp}$, $\gamma_{32}$, and $\gamma_{31}$, by keeping other parameters fixed as $\Omega_{pu}/(2\pi) = 5.0$ MHz, $\Omega_{pr}/(2\pi) = 0.1$ MHz and $\Gamma/(2\pi) = 6.0$ MHz.

Now, in Fig. 2, we have shown that the elastic atom-atom and atom-wall collisions produce the coherence dephasing ($\gamma_{12}$ and $\gamma_{21}$), whereas the inelastic atom-atom and atom-wall collisions produce the non-radiative population relaxation/exchange ($\Gamma_{21}$ and $\Gamma_{12}$) between the two ground states. To study the effects of coherence dephasing and non-radiative population relaxation on the EIT line shape and dispersion signals, we have considered $\Gamma_{21} = \Gamma_{12} = \Gamma_{pe}$ and $\gamma_{12} = \gamma_{21} = \gamma_{dp}$, where $\gamma_{dp}$ can be calculated as $\gamma_{dp} = \frac{\Gamma_{21}+\Gamma_{12}}{2}$ [18, 26]. We have further assumed that the decoherence effects due to elastic and inelastic collisions have the same contribution, i.e., $\Gamma_{pe} = \gamma_{dp}$, and the value of $\Gamma_{pe}/(2\pi) = \gamma_{dp}/(2\pi)$ is taken as 400 kHz [19]. Plot ($a$) of Fig. 3(i) shows the probe transmission as a function of the probe detuning ($\delta$) for $\Gamma_{pe}/(2\pi) = \gamma_{dp}/(2\pi) = 400$ kHz.

In addition to the elastic and inelastic collisional effects, the flight through broadening and phonon induced effects in solids can also produce the coherence dephasing in ground states. The non-radiative population relaxation may also arise from the thermal excitation/fluctuation [19]. In Refs. [23, 24], the authors have shown that the broadening of spectral line widths of the laser sources can also give rise to a decoherence in ground states. Since the EIT resonance is observed by the interaction of one or two laser fields with the atomic medium, so the spectral line width of the lasers plays an important role in the decoherence rates for both the ground and excited state. The laser line width variation may be due to fluctuations of the temperature and the current of a laser controller, and the different laser systems have different values of a laser line width. As a result, the value of the ground-state decoherence rate ($\Gamma_{pe}$ or $\gamma_{dp}$) increases, when all the natural phenomena are considered for the decoherence effects in the ground states. In Fig. 3(i),

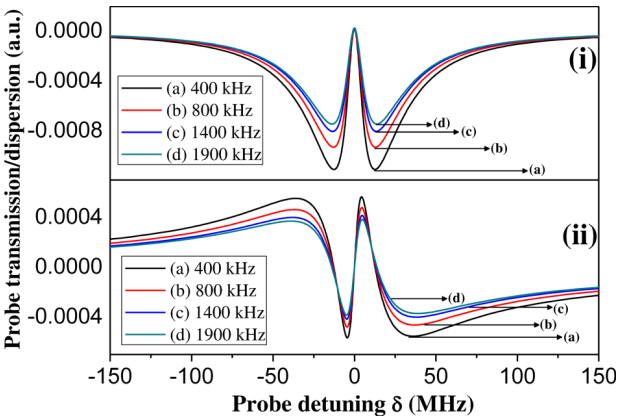


***Fig. 3.*** Variation of the probe transmission $\{\mathrm{Im}(\rho_{31})\}$ and dispersion $\{\mathrm{Re}(\rho_{31})\}$ signals as a function of the probe detuning ($\delta$) due to various ground-state decoherence effects

we have considered all other ground-state decoherence effects on the EIT signal by taking the value of $\Gamma_{pe}/(2\pi) = \gamma_{dp}/(2\pi)$ as 800 kHz (plot ($b$)), 1400 kHz (plot ($c$)) and 1900 kHz (plot ($d$)). From Fig. 3(i), we have found that the EIT peak height decreases, as the value of $\Gamma_{pe}/(2\pi) = \gamma_{dp}/(2\pi)$ increases. It is obtained that the EIT width (FWHM) increases and the EIT peak height decreases, as the value of the ground-state decoherence ($\Gamma_{pe}/(2\pi) = \gamma_{dp}/(2\pi)$) increases. Therefore, in order to achieve a good contrast and a narrow EIT signal, one needs to minimize the ground-state decoherence effects arising from the various natural and external phenomena. It is to be noted that the very small laser line width is one of the important criteria for getting a high contrast and a narrow EIT signal.

Similarly, in Fig. 3(ii), we plot the probe dispersion ($\mathrm{Re}(\rho_{31})$) as a function of the probe detuning ($\delta$) by considering the same set of values as in Fig. 3(i). We observe that the peak-peak height of a dispersion signal decreases, as the value of ground-state decoherence rate increases. Therefore, the dispersive signals become steeper, as the value of $\Gamma_{pe}/(2\pi) = \gamma_{dp}/(2\pi)$ becomes lower, i.e., the slope $\frac{dn(\omega_p)}{d\omega_p}$ of the dispersion curve increases, as the ground-state decoherence rate decreases. Hence, we can conclude that, in order to achieve steeper dispersion curves and to observe non-linear effects like "slow light" in an EIT medium, one needs to reduce the ground-state decoherence rate.

Now, to reduce the ground state decoherence rates, the most common method is the addition of a buffer

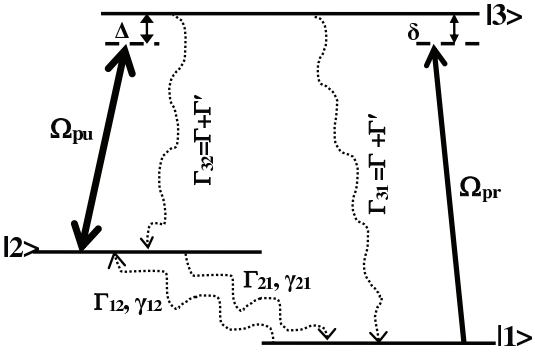


***Fig. 4.*** Representation of excited-state decoherence rates, where $\Gamma_{31} = \Gamma_{32} = \Gamma + \Gamma'$, and the ground-state decoherence rate as $\Gamma_{21} = \Gamma_{12} = \gamma_{12} = \gamma_{21}$

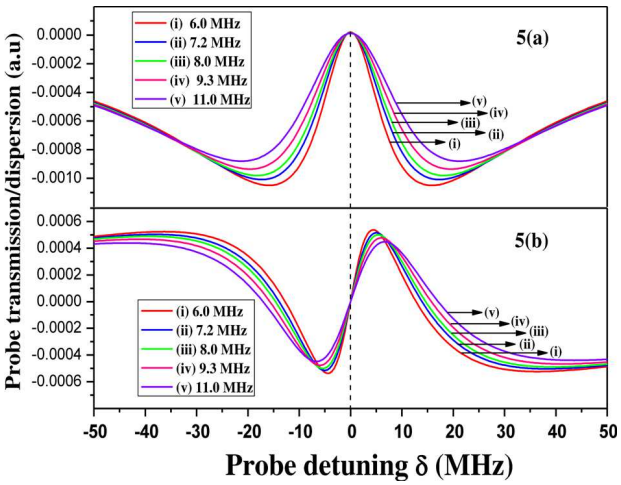


***Fig. 5.*** Effect of excited-state decoherence rates on the EIT and dispersion signals. Different values of $(\Gamma/2\pi)$ are 6.0 MHz (i), 7.2 MHz (ii), 8.0 MHz (iii), 9.3 MHz (iv), and 11.0 MHz (v)

gas inside the vapor cell. If a buffer gas is introduced in a pure atomic medium, then the velocity-changing coherence-preserving (VCCPs) collisions may help in reducing the ground-state decoherence rates. The higher buffer gas pressure also restricts the diffusion of alkali atoms from the atom-laser interaction region. As a result, the coherence of the alkali atoms in the interaction region will be long lived [15, 19, 20–23]. Therefore, the presence of a buffer gas reduces the ground-state decoherence rates and helps to obtain the narrow high-contrast EIT signal, as well as steep dispersive signals. The paraffin coating of the cell walls is another way to reduce the decoherence effects arising from the atom-wall collisions [22].

### *3.2. Excited-state decoherence effects*

The EIT line shapes and dispersive signals in a Λ-type system is affected not only by the ground-state decoherence rates, but also affected by the decoherence arising in the excited states. In Refs. [20–23, 26–29], the authors studied the various types of excited-state decoherence effects on the EIT signal. In addition to the spontaneous decays from the excited state (Γ), we represent the various excited-state decoherence effects by defining Γ′ (Fig. 4), which arises due to several phenomena like excited atom-atom collisions or buffer gas-induced collisions, laser line width fluctuations, non-radiative decays between the excited hyperfine levels, *etc.* In general, the spontaneous decay rates from the excited state are only considered in most of the theoretical calculation of EIT. Here, we will discuss all possible excited-state decoherence effects on the EIT and dispersion signals. In this section, we consider the ground-state decoherence rate as $\Gamma_{21} = \Gamma_{12} = \Gamma_{pe} = \gamma_{12} = \gamma_{21} = \gamma_{dp}$, and the fixed value of $\Gamma_{pe}/2\pi = \gamma_{dp}/2\pi$ is taken as 500 kHz in Eq. (8).

In plot (i) of Fig. 5, *a*, we consider only the spontaneous decay rate from the excited state as $\Gamma/2\pi = 6$ MHz. In Ref. [23], it was shown that the excited-state decoherence rate may be increased due to the collisions between excited atoms, excited atom and buffer gas atom/molecule, and to the spatial diffusion of the atoms out of the laser beams. It is also studied that the laser line width fluctuations make an additional decoherence effect in the excited states. But their contribution to the coherence loss is very small. We found in Ref. [29] that there also exist some non-radiative decays between the neighboring excited hyperfine levels (if we consider higher excited levels). In this work, we have considered all the possible excited-state decoherence effects, which increase the spontaneous decay rate of the excited state ($\Gamma/2\pi = 6$ MHz). In Eq. (8), we have substituted Γ by $\Gamma + \Gamma'$, where Γ′ arises due to the additional decoherence rates caused by various decoherence phenomena explained above.

In Fig. 5, we have studied and analyzed the probe transmission and dispersion signals for the different values of excited-state decoherence rates $(\Gamma/2\pi)$ starting from the spontaneous decay rate 6.0 MHz ((i) 6.0 MHz, (ii) 7.2 MHz, (iii) 8.0 MHz, (iv) 9.3 MHz

and (v) 11.0 MHz). Figure 5, *a* shows the plots of the probe transmission signals (EIT signals) with the different values of $\Gamma/2\pi$. It is seen that the strength of EIT signals decreases, as the value of $\Gamma/2\pi$ increases. We found that the EIT width and peak height, respectively, increases and decreases, as the value of $\Gamma/2\pi$ increases. At the same time, Fig. 5, *b* shows the plots of the probe dispersion signals with the different values of $\Gamma/2\pi$. Similarly, we have found that both the peak-peak height and the slope of dispersion signals decrease, as the value of $\Gamma/2\pi$ increases. When all the decoherence rates ($\Gamma'$) are added with the spontaneous decay rate ($\Gamma$), the effect of the excited-state decoherence on the EIT and dispersion signals is prominent in comparison with the EIT and dispersion signals observed, by only considering the spontaneous decay rate. Therefore, it is found that the good-contrast narrow EIT signal and the corresponding steep dispersion signals can be observed only when one can reduce the excited-state decoherence effects arising from the various decoherence phenomena. It is also found that the dispersive signal at the line center of the probe spectrum becomes less steep for the higher value of the excited-state decoherence rates, i.e., the slope $\frac{dn(\omega_p)}{d\omega_p}$ of the dispersion curve decreases, as the excited-state decoherence rate increases. In other words, to obtain a steeper dispersion curve, i.e., a reduction of the group velocity of a light pulse propagating through an EIT medium, we have to minimize the excited-state decoherence rates.

In Subsection (3.1), we have discussed that the presence of a buffer gas in an atomic vapor cell reduces the ground-state decoherence rates and helps to obtain a narrow high-contrast EIT signal [15, 19, 20–23]. When a buffer gas is introduced in a pure atomic medium, the VCCP collisions help to reduce the ground-state decoherence. But, at the same time, the buffer gas pressure produces an additional pressure broadening of the excited states and broadens the optical transition due to non-radiative effects. Therefore, the presence of a buffer gas affects both the ground- and excited-state decoherence rates, although the ground-state coherence preservation is much greater than the excited-state decoherence rate [20, 21]. As a result, the buffer gas inside a pure atomic vapor cell reduces the ground-state decoherence rates significantly, whereas the buffer gas-induced decoherence effect on the excited state is negligible.

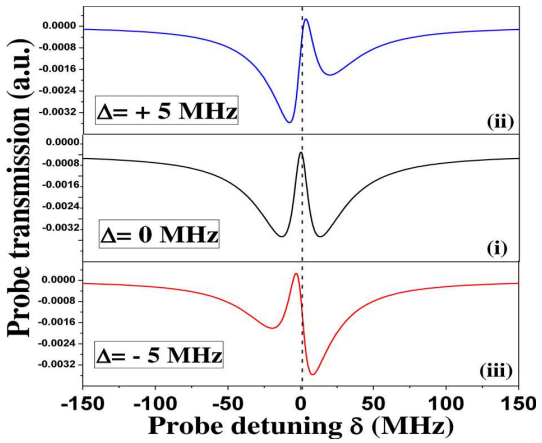


***Fig. 6.*** Effect of the pump detuning ($\Delta$) on the EIT position. $\Delta = 0$ MHz (i), $\Delta = +5$ MHz (ii), and $\Delta = -5$ MHz (iii)

Now, if we consider Eq. (7), where the pump detuning is arbitrary ($\Delta \neq 0$), we find that the EIT position shifts in the probe transmission signal, as the pump detuning changes. We plot the probe transmission $\{\mathrm{Im}(\rho_{31})\}$ with the probe detuning ($\delta$) for the different values of the pump detuning ($\Delta$): (i) $\Delta = 0$ MHz, (ii) $\Delta = +5$ MHz and (iii) $\Delta = -5$ MHz (Fig. 6). We observe that the EIT signal is symmetric at $\Delta = 0$, and it becomes asymmetric for the detuned position of a pump laser ($\Delta \neq 0$). Figure 6 shows that the shift of the EIT position is positive (blue shift) for the blue detuning of the pump field (Fig. 6-ii) and negative (red shift) for the red detuning of the pump field (Fig. 6-iii).

### *3.3. Effects of various parameters on atomic population*

The solutions of the population terms $\rho_{11}$, $\rho_{22}$ and $\rho_{33}$ at $\Delta = 0$ are obtained by solving the optical Bloch equations (1)–(6) at the weak probe limit,

$$\rho_{11} = \left[\frac{D_0\Gamma_{pe} + D_0\Gamma + 2\Gamma\Gamma_{pe}}{3D_0\Gamma_{pe} + D_0\Gamma + 4\Gamma\Gamma_{pe}}\right], \tag{9}$$

$$\rho_{22} = \left[\frac{2\Gamma\Gamma_{pe} + D_0\Gamma_{pe}}{3D_0\Gamma_{pe} + D_0\Gamma + 4\Gamma\Gamma_{pe}}\right], \tag{10}$$

$$\rho_{33} = \left[\frac{D_0\Gamma_{pe}}{3D_0\Gamma_{pe} + D_0\Gamma + 4\Gamma\Gamma_{pe}}\right], \tag{11}$$

where $\Gamma_{21} = \Gamma_{12} = \Gamma_{pe}$ and $D_0 = \frac{\Omega_{pu}^2}{2\gamma_{32}}$

It is quite evident from Eqs. (9) and (10) that, in the case of $\Omega_{pu} = \Omega_{pr} = 0$, the quasistationary solutions are $\rho_{11} = \rho_{22} = \frac{1}{2}$ and $\rho_{33} = 0$, when

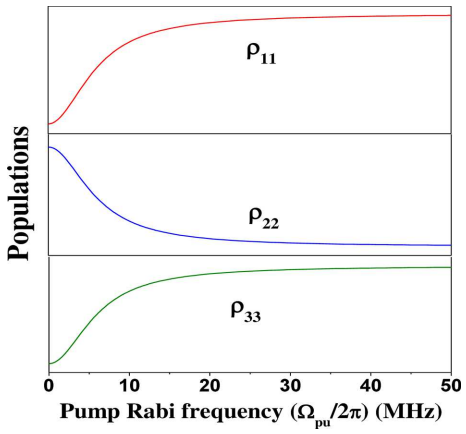


***Fig. 7.*** Variation of the populations ($\rho_{11}$, $\rho_{22}$ and $\rho_{33}$) at the pump Rabi frequency ($\Omega_{pu}$). The fixed values are taken as $\Gamma/2\pi = 6.0$ MHz, $\Gamma_{21}/2\pi = \Gamma_{12}/2\pi = \Gamma_{pe}/2\pi = 1.0$ MHz, and $\gamma_{32}/2\pi = 6.5$ MHz

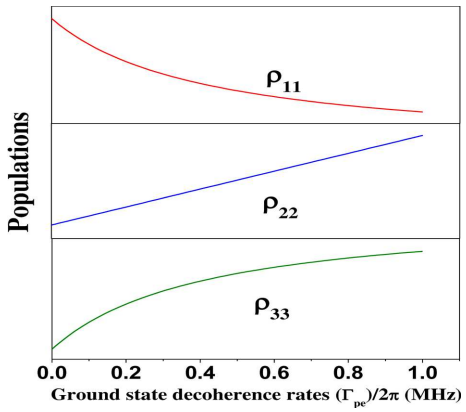


***Fig. 8.*** Variation of the populations ($\rho_{11}$, $\rho_{22}$ and $\rho_{33}$) with ground-state decoherence rates ($\Gamma_{pe}$). The fixed values are taken as $\Omega_{pu}/2\pi = 5.0$ MHz, $\Gamma/2\pi = 6.0$ MHz, and $\gamma_{32}/2\pi = = 6.5$ MHz

$\Gamma_{21} = \Gamma_{12} = \Gamma_{pe} \neq 0$. From Eqs. (9) and (10), we have found that the values of $\rho_{11}$ and $\rho_{22}$ satisfy the boundary condition $\rho_{11} + \rho_{22} = 1$ in the ideal case where $\Gamma_{21} = \Gamma_{12} = \Gamma_{pe} = 0$. Now, we study the dependence of atomic populations on the pump Rabi frequency ($\Omega_{pu}$) and ground-state decoherence rates ($\Gamma_{pe}$) in Figs. 7 and 8, respectively.

In Fig. 7, we observe that the population of level $|1\rangle$ starts increasing, as one keeps on increasing the pump Rabi frequency ($\Omega_{pu}$). Simultaneously, the population of level $|2\rangle$ keeps on decreasing. This is expected, as the probe laser connects the levels $|1\rangle$ to $|3\rangle$, and the pump laser connects the levels $|2\rangle$ to $|3\rangle$. Hence, the population of level $|2\rangle$ keeps on decreasing, and the populations of levels $|1\rangle$ and $|3\rangle$ keeps on increasing with an increase in $\Omega_{pu}$.

When we increase the values of $\Gamma_{pe}$ in Eqs. (9)–(11), it is found that the population of level $|1\rangle$ decreases, and the population of level $|2\rangle$ increases (Fig. 8). It may be due to the reason that a few atoms through some non-radiative processes like atom-atom and atom-wall collisions are removed from the level $|1\rangle$ and reach level $|2\rangle$. At the same time, since the pump laser is also connected between the levels $|2\rangle$ and $|3\rangle$, then more and more number of atoms will be pumped into the higher excited level $|3\rangle$ from the level $|2\rangle$, by resulting in the effective increase in the population of level $|3\rangle$.

## 4. Conclusion

We have analytically found the solutions of the optical Bloch equations for a simple three-level $\Lambda$-type system in two co-propagating laser fields, where the relaxation of populations of the ground states is taken into account. The probe transmissions $\{\mathrm{Im}(\rho_{31})\}$ and the probe dispersions $\{\mathrm{Re}(\rho_{31})\}$ are calculated and then plotted for various decoherence effects involved in the ground and excited levels. We have found that the EIT line width increases and the peak height decreases with an increase in both ground- and excited-state decoherence rates. The dispersive signals are steeper and higher contrast for the lower values of both ground- and excited-state decoherence rates. We have also discussed the effect of a buffer gas in a vapor cell, which helps one to obtain the narrow high-contrast EIT and steep dispersion signals by reducing the ground-state decoherence rates. The various physical phenomena behind the various types of decoherence effects arising in the ground and excited levels are discussed elaborately. In addition to the decoherence effects, we have studied the effect of the pump detuning on the EIT line shapes and have shown that the central symmetric EIT peak becomes asymmetric, as the pump detuning changes. The variations of atomic populations with the pump Rabi frequency and the ground-state decoherence rates are also studied. Our results are well consistent with the earlier theoretical and experimental results, and we believe that the detailed analysis of the EIT and dispersive signals under various decoherence effects provides a better understanding on the broadening of EIT and dispersive signals.

*R. Hazra acknowledges Aliah University for providing the University Research Scholar Fellowship. Md.M. Hossain acknowledges Science and Engineering Research Board (SERB, DST, Govt. of India) for sanctioning the start-up research grant (FTP/PS-206/2013) through the Early Career Research Award (ECRA) and DHESTBT (Govt. of West Bengal) for sanctioning a research project (Ref. No. 249 (Sanc.)/ST/P/S&T/16G-26/2017).*

1. M.O. Scully, M.S. Zubairy. *Quantum Optics* (Cambridge Univ. Press, 1999).
2. S.E. Harris. Electromagnetically induced transparency. *Phys. Today* **50** (7), 36 (1997).
3. J.P. Marangos. Topical review electromagnetically induced transparency. *J. Mod. Opt.* **45**, 471 (1998).
4. M. Fleischhauer, A. Imamoglu, J.P. Marangos. Electromagnetically induced transparency: Optics in coherent media. *Rev. Mod. Phys.* **77**, 633 (2005).
5. A.M. Akulshin, S. Barreiro, A. Lezama. Electromagnetically induced absorption and transparency due to resonant two-field excitation of quasidegenerate levels in Rb vapor. *Phys. Rev. A* **57**, 2996 (1998).
6. A. Lipsich, S. Barreiro, A.M. Akulshin, A. Lezama. Absorption spectra of driven degenerate two-level atomic systems. *Phys. Rev. A* **61**, 053803 (2000).
7. A.V. Taichenachev, A.M. Tumaikin, V.I. Yudin. Electromagnetically induced absorption in a four-state system. *Phys. Rev. A* **61**, 011802 (2000).
8. M. Kwon, K. Kim, H.S. Moon, H.D. Park, J.B. Kim. Electromagnetically induced absorption spectra depending on intensities and detunings of the coupling field in Cs vapour. *J. Phys. B* **34**, 2951 (2001).
9. J. Kitching, S. Knappe, L. Hollberg. Miniature vapor-cell atomic-frequency references. *Appl. Phys. Lett.* **81**, 553 (2002).
10. A.H. Safavi-Naeini, T.P.M. Alegre, J. Chan, M. Eichenfield, M. Winger, Q. Lin, J.T. Hill, D.E. Chang, O. Painter. Electromagnetically induced transparency and slow light with optomechanics. *Nature.* **472**, 69 (2011).
11. P.W. Milonni. *Fast Light, Slow Light and Left Handed Light* (Taylor and Francis Group, 2005).
12. M. Fleischhauer, M.D. Lukin. Dark-State polaritons in electromagnetically induced transparency. *Phys. Rev. Lett.* **84**, 5094 (2000).
13. L.M. Duan, M.D. Lukin, J.I. Cirac, P. Zoller. Long-distance quantum communication with atomic ensembles and linear optics. *Nature* **414**, 413 (2001).
14. H. Lee, M. Fleischhauer, M.O. Scully. Sensitive detection of magnetic fields including their orientation with a magnetometer based on atomic phase coherence. *Phys. Rev. A* **58**, 2587 (1998).
15. M.M. Hossain, S. Mitra, B. Ray, P.N. Ghosh. High contrast electromagnetically induced transparency in a nitrogen filled Rb vapour cell. *Laser Phys.* **19**, 2008 (2009).
16. A. Javan, O. Kocharovskaya, H. Lee, M.O. Scully. Narrowing of electromagnetically induced transparency resonance in a Doppler-broadened medium. *Phys. Rev. A* **66**, 013805 (2002).
17. H. Lee, Y. Rostovtsev, C.J. Bednar, A. Javan. From laser-induced line narrowing to electromagnetically induced transparency: Closed system analysis. *Appl. Phys. B* **76**, 33 (2003).
18. Z. Lian-shui, Y. Li-jun, L. Xiao-li, Z. Zhong-hong, G. Qinglin. Spectral line narrowing effect induced by atomic coherence in a three-level $\Lambda$ system. *Optoelectron. Lett.* **3**, 5 (2007).
19. S. Mitra, M.M. Hossain, B. Ray, P.N. Ghosh, S. Cartaleva, D. Slavov. On line shape of electromagnetically induced transparency in a multilevel system. *Opt. Commun.* **283**, 1500 (2010).
20. Z.F. Hu, C.G. Du, Y.Z. Wang. Buffer-gas-induced narrowing of electromagnetically induced transparent spectra for an open system. *J. Mod. Opt.* **53**, 4 (2006).
21. E.E. Mikhailov, I. Novikova, Y.V. Rostovtsev, G.R. Welch. Buffer-gas-induced absorption resonances in Rb vapor. *Phys. Rev. A* **70**, 033806 (2004).
22. E.E. Mikhailov, V.A. Sautenkov, Y.V. Rostovtsev, G.R. Welch. Absorption resonance and large negative delay in rubidium vapor with a buffer gas. *J. Opt. Soc. Am. B* **21**, 2 (2004).
23. M. Erhard, H. Helm. Buffer-gas effects on dark resonances: Theory and experiment. *Phys. Rev. A* **63**, 043813 (2001).
24. G. Rui-Min, X. Feng, L. Cheng, Z. Yu, C. Xu-Zong. Dependence of electromagnetically induced transparency on laser linewidth. *Chin. Phys. Lett.* **20**, 9 (2003).
25. E. Figueroa, F. Vewinger, J. Appel, A.I. Lvovsky. Decoherence of electromagnetically induced transparency in atomic vapor. *Opt. Lett.* **31**, 17 (2006).
26. J. Wang. Decoherence effects in an electromagnetically induced transparency and slow light experiment. *Phys. Rev. A* **81**, 033841 (2010).
27. J. Ghosh, R. Ghosh, F. Goldfarb, J.-L. L. Gouet, F. Bretenaker. Analysis of electromagnetically induced transparency and slow light in a hot vapor of atoms undergoing collisions. *Phys. Rev. A* **80**, 023817 (2009).
28. J. Vanier, A. Godone, F. Levi. Coherent population trapping in cesium: Dark lines and coherent microwave emission. *Phys. Rev. A* **58**, 2345 (1998).
29. V. Wong, R.W. Boyd, C.R. Stroud, jr., R.S. Bennink, A.M. Marino. Thirteen pump-probe resonances of the sodium D1 line. *Phys. Rev. A* **68**, 012502 (2003).
30. O. Katz, O. Peleg, O. Firstenberg. Coherent coupling of alkali atoms by random collisions. *Phys. Rev. Lett.* **115**, 113003 (2015).
31. H. Gao, M. Rosenbery, J. Wang, H. Batelaan. Experimental studies of light propagation and storage in warm atomic gases. *J. Phys. B* **38**, 1857 (2005).

32. G. Kazakov, B. Matisov, A. Litvinov, I. Mazets. Coherent population trapping in a finite-size buffer-less cell. *J. Phys. B* **40**, 3852 (2007).

33. Y. Pashayan-Leroy, C. Leroy, A. Sargsyan, A. Papoyan, D. Sarkisyan. Electromagnetically induced transparency: the thickness of the vapor column is of the order of a light wavelength. *J. Opt. Soc. Am. B* **24**, 1829 (2007).

34. A. V. Taichenachev, V. I. Yudin, R. Wynands, M. Stahler, J. Kitching, L. Hollberg. Theory of dark resonances for alkali-metal vapors in a buffer-gas cell. *Phys. Rev. A* **67**, 033810 (2003).

35. A.I. Parkhomenko, A.M. Shalagin. Ground-state pump-probe spectroscopy. *J. Exp. Theor. Phys.* **105**, 1095 (2007).

36. Stephen Colby Rand, *Lectures on Light: Nonlinear and Quantum Optics using the Density Matrix* (Oxford Univ. Press, 2010).

37. L. Hau, S.E. Harris, Z. Dutton, C.H. Behroozi. Light speed reduction to 17 metres per second in an ultracold atomic gas. *Nature.* **397**, 594 (1999).

38. S.E. Harris, J.E. Field, A. Imamoglu. Nonlinear optical processes using electromagnetically induced transparency. *Phys. Rev. Lett.* **64**, 1107 (1990).

39. S.E. Harris, J.E. Field, A. Kasapi. Dispersive properties of electromagnetically induced transparency. *Phys. Rev. A* **46**, 29 (1992).

Received 27.07.18

*Р. Хазрі, Мд.М. Хоссейн*

ВИВЧЕННЯ НАСЕЛЕНОСТІ АТОМІВ, ЕЛЕКТРОМАГНІТНОІНДУКОВАНОЇ ПРОЗОРОСТІ І ДИСПЕРСІЙНИХ СИГНАЛІВ У СИСТЕМІ Λ-ТИПУ З РІЗНИМИ ЕФЕКТАМИ ДЕКОГЕРЕНТНОСТІ

Р е з ю м е

Теоретично досліджені населеності атомів, електромагнітноіндукована прозорість (ЕІП) і дисперсія в трирівневій системі Λ-типу. Побудовано рівняння для матриці щільності з урахуванням релаксації в основному стані і вирішені рівняння Блоха в наближенні слабкого тестуючого поля. Для основного і збудженого станів вивчено вплив декогерентності на форму лінії при ЕІП і на дисперсійні сигнали. Знайдено, що ширина лінії при ЕІП збільшується і висота піка зменшується при зростанні швидкості декогерентності. З іншого боку, при малих швидкостях декогерентності дисперсійні сигнали крутіше і більше контрастні в основному і збудженому станах. Проаналізовано зміну населеності рівнів енергії атомів при накачуванні з частотою Рабі та швидкість декогерентності в основному стані.